The Journal of Neuroscience, April 15, 1996, 16(8):2421–2429

Inwardly Rectifying K^+ Channels that May Participate in K^+ Buffering Are Localized in Microvilli of Schwann Cells

Huaiyu Mi,[1] Thomas J. Deerinck,[2] Maggie Jones,[1] Mark H. Ellisman,[2] and Thomas L. Schwarz[1]

[1]Department of Molecular and Cellular Physiology, Beckman Center, Stanford University Medical Center, Stanford, California 94305, and [2]National Center for Microscopy and Imaging Research, Department of Neurosciences, School of Medicine, University of California at San Diego, La Jolla, California 92093

The presence of K^+ channels on the Schwann cell plasma membrane suggests that Schwann cells may participate actively during action potential propagation in the peripheral nervous system. One such role for Schwann cells may be to maintain a constant extracellular concentration of K^+ in the face of K^+ efflux from a repolarizing axon. This buffering is likely to involve the influx of K^+ through inward rectifying K^+ channels. The molecular cloning of these genes allowed us to examine their expression and localization in Schwann cells in detail. In this study, we demonstrate the expression of two inward rectifying K^+ channels, IRK1 and IRK3, in adult rat sciatic nerve. Immunocytochemistry using a polyclonal antibody against these proteins showed that the channels were highly localized at nodes in sciatic nerve. By immunoelectron microscopy, the nodal staining was shown to be concentrated in the microvilli of Schwann cells (also called nodal processes). The large surface area of the microvilli and their presence in the nodal space suggest involvement with ionic buffering. Thus, IRK1 and IRK3 are well suited to K^+ buffering by virtue of both their biophysical properties and their localization. The restricted distribution of the inward rectifying K^+ channels also provides an example of the highly regulated localization of ion channels to their specialized membrane domains. In the Schwann cell, where the nodal processes are a minute fraction of the total cell membrane, a potent mechanism must be present to concentrate the channels in this structure.

Key words: potassium channel; Schwann cell; node of Ranvier; inward rectifier; IRK1; localization; microvilli; buffering; myelin

Schwann cells form myelin sheaths that serve as an insulator for peripheral nerve axons. The close relation between Schwann cells and axons has led to the consideration that Schwann cells may be involved in more active roles, such as determining the domains of axons in which ion channels will be segregated (Ellisman, 1979; Rosenbluth, 1979; Wiley-Livingston and Ellisman, 1980, 1981; Black et al., 1990), and regulating the ionic environment for the axons (Villegas, 1981). The discovery of ion channels in the membrane of Schwann cells, as well as in astrocytes in the CNS (for review, see Barres et al., 1990a; Chiu, 1991; Ritchie, 1992), further supports the idea that Schwann cells may participate actively in neuronal signaling. K^+ currents that have been reported in cultured or acutely dissociated Schwann cells include delayed rectifying, inward rectifying, transient A type, and Ca^{2+}-activated currents (Chiu et al., 1984; Shrager et al., 1985; Howe and Ritchie, 1988; Konishi, 1989; Wilson and Chiu, 1990a,b; Verkhratsky et al., 1991).

One hypothesis to explain why Schwann cells possess these K^+ channels is that Schwann cells may participate in a process called "K^+ buffering," a concept originally put forward for glial cells of the CNS (Orkand et al., 1966). Subsequently, this hypothesis was extended to the Schwann cells of the peripheral nervous system (Chiu, 1990) where, during the action potential, K^+ flows out of axons to repolarize the membrane. This efflux could cause, however, an accumulation of extracellular K^+, which in turn would decrease the excitability of the axonal membrane. The K^+ buffering hypothesis postulates that Schwann cells provide for the quick and efficient removal of these ions from the extracellular space by taking up K^+. Two practical mechanisms have been proposed: "spatial buffering" (Orkand et al., 1966) and "K^+ accumulation" (Bevan et al., 1985). In "spatial buffering," K^+ would enter the Schwann cells in a region of high external K^+ and flow intracellularly to other regions of the cell. In "K^+ accumulation," K^+ would enter the Schwann cell together with Cl^- and water and accumulate near the site of entry. Later, K^+ would be expected to exit the Schwann cell and be recaptured by the axon.

For K^+ buffering to occur by either mechanism, one would expect K^+ channels on Schwann cells in the vicinity of the nodes. By patch clamping on Schwann cells in the vicinity of nodes, Wilson and Chiu (1990b) were able to record two types of K^+ currents: delayed rectifying outward current and inward rectifying current. Both currents were concentrated at the nodes rather than at the perinuclear region of the Schwann cell. By molecular cloning and immunocytochemistry, we determined that a particular voltage-activated K^+ channel, Kv1.5, is in the outer Schwann cell membrane near the node (Mi et al., 1995). However, Kv1.5 channels were still at some distance from the axonal membranes. Moreover, they require a depolarization to be opened and, at depolarized potentials, K^+ efflux would be favored. Thus, Kv1.5 is not an ideal candidate for mediating the influx of K^+ into the Schwann cell. Inward rectifying K^+ channels, which are conduct-

Received Aug. 30, 1995; revised Jan. 11, 1996; accepted Jan. 17, 1996.

This work was supported by National Institutes of Health Grants GM42376 and HL48636 to T.L.S. and RR04050, NS14718, and NS26739 to M.H.E. Both laboratories contributed equally to this work. We thank Drs. Lily Jan, Yoshihisa Kurachi, and Carol Vandenberg for kindly providing cDNA clones. We also thank Ms. I. Inman for outstanding technical assistance and Dr. B. Barres for helpful discussions.

Correspondence should be addressed to Thomas L. Schwarz, Department of Molecular and Cellular Physiology, Beckman Center, Stanford University Medical Center, Stanford, CA 94305.

ing at resting potentials and favor inward currents, would be more plausible candidates to perform this hypothetical role.

The cloning and expression of the first genes for inward rectifying K^+ channels, ROMK1 and IRK1 (Ho et al., 1993; Kubo et al., 1993a), have led to the uncovering of numerous homologs in mice, rats, and humans, including GIRK1 (Kubo et al., 1993b), CIR (Krapivinsky et al., 1995) (which is also called KATP in Ashford et al., 1994), IRK2 (Koyama et al., 1994; Takahashi et al., 1994), and IRK3 (Morishige et al., 1994) [also called HIRK1 in Makhina et al. (1994), hIRK2 in Tang and Yang (1994), HIR in Perier et al. (1994), and Bir11 in Bond et al. (1994)]. IRK1, IRK2, and IRK3 share ~70% identity and may be classified together into an IRK subfamily. In the recently proposed nomenclature of Doupnik et al. (1995), these are called Kir2.1, Kir2.2, and Kir2.3, respectively. The IRK (Kir2.0) subfamily is structurally and physiologically distinct from the more distantly related ROMK1, CIR, and GIRK1 genes (representatives of the Kir1.0 and Kir3.0 subfamilies). When expressed in *Xenopus* oocytes, all IRK subfamily channels show strong inward rectification and sensitivity to Cs^+ and Ba^{2+}. These properties are similar to those described in glial inward rectifying K^+ channels (Brew et al., 1986; Brismar and Colins, 1989; Newman, 1993).

In the present study, we report that two members of the IRK family, IRK1 and IRK3, are expressed in sciatic nerve. Immunocytochemistry demonstrates that these channels are highly concentrated at the node of Ranvier in Schwann cells, mostly on microvilli that fill much of the nodal cleft. This localization strongly supports the hypothesis that Schwann cells carry out a K^+-buffering role and suggests that IRK1 and IRK3 are likely to mediate K^+ uptake.

MATERIALS AND METHODS

Molecular cloning. To clone IRK-like channels from rat sciatic nerve, degenerate oligos were synthesized corresponding to the sequence of murine IRK1 near the N and C termini. The N-terminal primers were: 5′ primer GA(A/G)GA(A/G)GA(C/T)GGIATGAA(A/G)(C/T)T (amino acids 15–21; Kubo et al., 1993a), and 3′ primer CCA(A/G)AAIAC(A/G)CAICC(A/G)AA(A/G)AA (amino acids 98–104). The C-terminal primers were: 5′ primer ACIGCIATGACIACICA(A/G)TG (amino acids 305–311), and 3′ primer GC(C/T)TG(A/G)TT(A/G)TGIA(A/G)(A/G)TCIAT (amino acids 407–412). mRNA was extracted from rat sciatic nerve as described previously (Mi et al., 1995) and subjected to reverse transcription (RT)-PCR (Sambrook et al., 1989). Each of 40 cycles of PCR consisted of 1 min at 94°C, 1 min at 42°C, and 1 min at 72°C. Because the yields were low, an internal primer for each pair was used to further amplify the PCR product. The sequence for the internal primer for the N-terminal fragment was CA((A/G)AAIATIACIA(A/G)CATCCA (amino acids 83–89), and that for the C-terminal fragment was GA(A/G)GA(A/G)AA(A/G)CA(C/T)TA(C/T)TA(C/T)AA(A/G)GT (amino acids 332–338). Twenty-five cycles of PCR were performed with the internal and 5′ primers for the N-terminal and with the internal and 3′ primers for the C-terminal to yield 225 and 243 bp fragments, respectively. Both were subcloned into *Eco*RV-digested Bluescript vector (Stratagene, La Jolla, CA) and sequenced. Additional primers were then used to obtain the middle of the rat IRK1 (rIRK1) sequence by RT-PCR as described above: 5′ primer ACATCTTTACTACCTGTGTGG (amino acids 71–77) and 3′ primer AGTCTCTGGCACTACAAAGGG (amino acids 354–360). The three PCR products indicated a high degree of homology to the published murine sequence for IRK1 and covered 93% of the predicted open reading frame of the rat homolog.

Transcripts analysis. Rat brain mRNA (3 μg) and rat sciatic nerve total RNA (10 μg) were analyzed on blots as described previously (Mi et al., 1995). The mouse IRK1 clone (kindly provided by Dr. Lily Jan) was used as a probe in 50% formamide, 5× SSPE, 5% SDS, 5× Denhardt's solution, and 330 μg/ml salmon sperm DNA at 45°C overnight. The blot was washed twice at 2× SSC at 55°C with 30 min each and was exposed for 40 hr.

When rIRK1 was used as the probe, 2 μg of brain and sciatic nerve mRNA was analyzed at high stringency (Mi et al., 1995). The same blot was reprobed at 50°C with a human IRK3 clone (the HIR clone, kindly provided by Dr. Carol Vandenberg; see Perier et al., 1994), washed in 0.5× SSC at 55°C, and exposed for 48 hr. Similarly, the murine IRK2 clone (kindly provided by Dr. Yoshihisa Kurachi) was used to probe for IRK2 expression, but no band could be detected in sciatic nerve mRNA after exposing the film for 7 d.

Antibody production. Peptides were made corresponding to sequences from both the N- and C-terminal regions of IRK1. The sequence for the N-terminal peptide was NGKSKVHTRQQCRSRFVK (amino acids 32–49), and that for the C-terminal peptide was RFHKTYEVPNTPLCSARD (amino acids 343–360). These regions are identical between mouse IRK1 and rIRK1. The coupling of the peptides to thyroglobulin, antibody production, and affinity purification were as described previously (Mi et al., 1995). Only the N-terminal peptide produced a successful antiserum (as judged by its ability to stain transfected COS cells; see below), which is referred to hereafter as anti-IRK.

Western blot. Forty adult sciatic nerves or one adult rat brain was homogenized in a Dounce homogenizer with 10 ml of SHEEP buffer (0.32 M sucrose, 10 mM HEPES, pH 7.0, 1 mM EGTA, 0.1 mM EDTA, and 0.5 mM phenylmethylsulfonyl fluoride). The homogenate was then spun at 1000 × *g* for 10 min, and the supernatant was recovered. Supernatant from sciatic nerve (20 μl) or from brain (4 μl) was mixed with equal volumes of 2× loading buffer, heated at 100°C for 10 min, and fractionated on a 10% acrylamide-SDS gel. The proteins were transferred to nitrocellulose that was incubated overnight at 4°C with 15 mM Tris-HCl, pH 7.5, 0.13 M NaCl, 10 mM EDTA, pH 7.0, 1% Tween 20, and 0.1% gelatin. The filter was then incubated at room temperature for 1 hr with 5% normal goat serum, 1% bovine serum albumin, 5% nonfat milk in PBT (0.1% Tween-20 in PBS). Affinity-purified anti-IRK was diluted 1:100 in PBT and incubated at room temperature for 2 hr with the filters, which were then washed six times with PBT for a total of 1.5–2 hr at room temperature. The immunoreactivity was visualized by enhanced chemoluminescence with an ECL kit (Amersham, Arlington Heights, IL) and the manufacturer's suggested protocol.

Immunocytochemistry and immunoelectron microscopy. Immunofluorescent and immunoelectron microscopy detection was carried out as described previously (Mi et al., 1995). For immunofluorescence, fixed and teased sciatic nerves were incubated in affinity-purified anti-IRK antibody at a dilution of 1:40 at 4°C overnight followed by an affinity-purified goat anti-rabbit IgG–fluorescein conjugate (diluted at 1:200 in working buffer, Vector Laboratories, Burlingame, CA). Fluorescence and transmitted light images were obtained with an MRC-1000 confocal imaging system (Bio-Rad, Hercules, CA). For immunoelectron microscopy, sciatic nerves were fixed in 0.5% glutaraldehyde and 2% formaldehyde and incubated in the anti-IRK antibody at a dilution of 1:40 at 4°C overnight. Detection was accomplished using an ABC peroxidase kit (Vector) as described previously (Mi et al., 1995). Electron micrographs of thin sections (80 nm) were recorded with a JEOL 100cx electron microscope at 80 keV, and semithick section (1 μm) were recorded with a JEOL 4000ex intermediate voltage electron microscope operating at 400 keV. Stereo pair images of semithick sections were generated by tilting the sample ±5°.

The procedures for COS cell transfection and staining were described previously (Mi et al., 1995). Murine IRK1 and hIRK3 cDNA in pCDNA1 vectors (Invitrogen, San Diego, CA) were used for the transfection. Forty-eight hours after the transfection, the cells were fixed by 4% formaldehyde and stained with anti-IRK antibody at a dilution of 1:40.

RESULTS

Identification of rIRK1 in adult rat sciatic nerve

When the mouse IRK1 gene (Kubo et al., 1993a) was used to probe mRNA from rat sciatic nerves and brain at low stringency (Fig. 1*A*), a transcript was detected in both tissues that was comparable in size (5.5 kb) to the IRK1 transcript in mouse (Kubo et al., 1993a). Other bands were also detected that may correspond to nonspecific binding or additional homologs of IRK1 (see below).

By RT-PCR with degenerate oligonucleotides, we were able to isolate from sciatic nerve mRNA partial clones for rIRK1 in the N- and C-terminal regions. PCR primers were synthesized to sequences from each of these clones, and the middle part of the clone was thereby obtained. Together, these clones corresponded

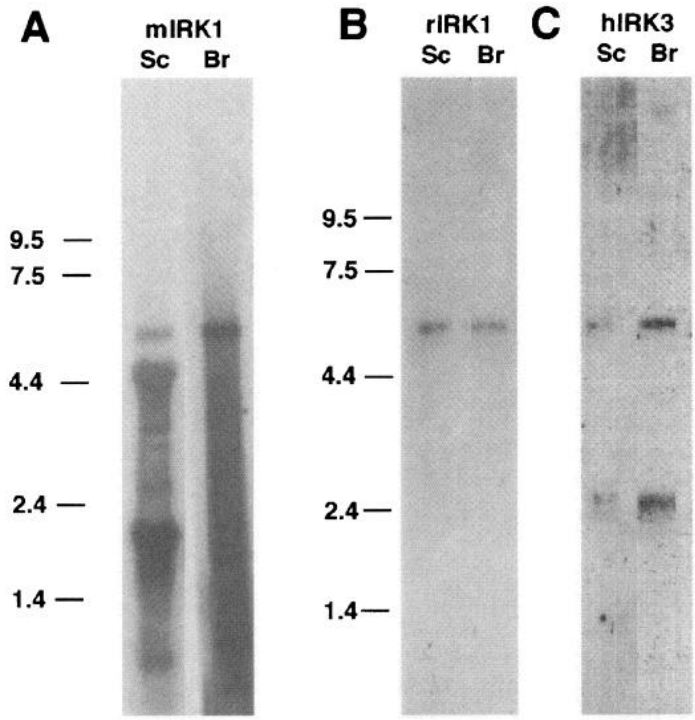

Figure 1. IRK family transcripts in sciatic nerve and brain. *A*, Rat sciatic total RNA (*Sc*) and brain mRNA (*Br*) were hybridized with the mouse IRK1 clone at a relatively low stringency (see Materials and Methods). A 5.5 kb transcript for IRK1 was detected in both tissues despite the nonspecific hybridization to ribosomal and other RNA at this low stringency. *B*, mRNA from rat sciatic nerve (*Sc*) and brain (*Br*) were hybridized at high stringency with the rat IRK1 clone representing amino acids 71–360, and a single 5.5 kb transcript was detected in both tissues. *C*, The same blot as in *B* was reprobed with a human IRK3 clone. A 2.7 kb and a 5.5 kb band were detected in both tissues, but with lower expression in sciatic nerve than brain. The positions of RNA size standards (in kb) are marked.

to 93% of the sequence of IRK1 (amino acids 15–412) and revealed that the mouse and rat IRK1 genes shared 99.2% amino acid identity and 94% nucleotide identity. The amino acid differences that were detected in the rat were Ala substituting for Thr at murine position 115, Glu for Val at 118, and Cys for Tyr at 336. rIRK1 also lacks one Glu in a stretch of Glu between amino acids 386 and 389. We were unable to isolate a full-length cDNA for rIRK1 from a cultured Schwann cell library (Monuki et al., 1989); the absence of the clone may reflect a difference between cultured and mature Schwann cells (see also Mi et al., 1995). The partial clone of rIRK1 was used in a high-stringency Northern blot of adult rat sciatic nerve (Fig. 1*B*). A single band of 5.5 kb was present, indicating that rIRK1 is expressed in this tissue.

Expression of IRK3 in adult rat sciatic nerve

We examined the expression in sciatic nerve of the closely related IRK3 gene (also called HIR) (Morishige et al., 1994; Takahashi et al., 1994) by Northern blot using a human IRK3 clone. Both 2.7 and 5.5 kb bands were detected (Fig. 1*C*), similar to what had been reported for brain of other species (Morishige et al., 1994; Perier et al., 1994; Tang and Yang, 1994). The expression level of IRK3, however, was considerably lower in sciatic nerve than in brain (Fig. 1*C*). Although others have speculated that the 5.5 kb band may be attributable to cross-reactivity with the 5.5 kb rIRK1 transcripts (Tang and Yang, 1994), this cannot be the case here because rIRK1 was equally abundant in rat sciatic nerve and brain (Fig. 1*B*), and this is not true for the 5.5 kb transcript seen with IRK3. The two transcripts, therefore, are likely to arise from IRK3 by alternative promotor choice or RNA processing. The murine IRK2 cDNA was also used as a probe and, although a transcript in rat brain was recognized, no IRK2 transcripts were detected in sciatic nerve.

Antibody production

An antibody was raised against a peptide corresponding to a sequence from the N-terminal region of IRK1 (see Materials and Methods). This peptide falls in a region with considerable similarity among IRK1, IRK2, and IRK3 (Fig. 2*B*) but no homology to the more distantly related inward rectifiers. After affinity purification, the serum (called anti-IRK) was used to stain COS cells transfected with either mouse IRK1 or human IRK3. The antiserum showed strong staining on COS cells transfected with either clone (Fig. 2*A*). The staining could be blocked by preincubation of antibody with the peptide, and this staining was not seen with the preimmune antiserum or with nontransfected COS cells. Because of the similarities of sequence, it is likely that the antibody will recognize IRK2 as well, although we have not tested this.

The specificity of our antiserum was examined on Western blots. Two bands of 73 and 75 kDa were detected in proteins extracted from sciatic nerve (Fig. 2*C*, *lane 1*). Staining of both bands was prevented when the antiserum was preabsorbed with peptide antigen or when no primary antiserum was added (Fig. 2*C*, *lanes 3* and *4*, respectively). The sizes of the IRK1 and IRK3 proteins that are predicted from the cDNA sequences are 47 and 49 kDa. The discrepancy in size could be attributable to 26 kDa of glycosylation: the 73 kDa band may correspond to IRK1 protein, and the 75 kDa band to IRK3 protein. Their respective transcript levels (Fig. 1) are consistent with the greater abundance of the putative IRK1 protein. In brain there is a third band of ~81 kDa (Fig. 3, *lane 2*) the nature of which is not known at present. Thus, the sequence of the immunogen, the staining of transfected COS cells, and the results of the Western blots are consistent with a characterization of the antiserum as a reagent suitable for detecting members of the IRK family.

Localization of IRK channels in peripheral nerves

Anti-IRK was used to localize the IRK family of channels in teased preparations of adult rat sciatic nerve. Immunoreactivity was consistently concentrated near nodes of Ranvier (Fig. 3*A*,*C*), which could be identified with transmitted light microscopy (Fig. 3*B*). In each experiment, >80% of the nodes in the preparation were stained, and when the nerve fibers were teased apart particularly well, >90% were stained. The occasional unstained node may result from poor accessibility of the antibodies.

Although this distribution was reminiscent of Kv1.5 channels (Mi et al., 1995), on close examination the two could be distinguished. Kv1.5, in addition to its presence at the node, is present in the canaliculi of the Schwann cells, a specialization of the outer layer of the internode that connects the perinuclear region with the node (Mi et al., 1995). These structures were not stained with anti-IRK. Furthermore, in Kv1.5 staining there was a gap between the two stained surfaces that face one another across the nodal gap. Electron microscopy demonstrated that this was because the Kv1.5 channel immunoreactivity was on the curved, outer shoulder of Schwann cells that border the node, but was not apparent on the microvilli that fill the nodal gap. This gap was not observed in the preparations stained for IRK channels and under higher

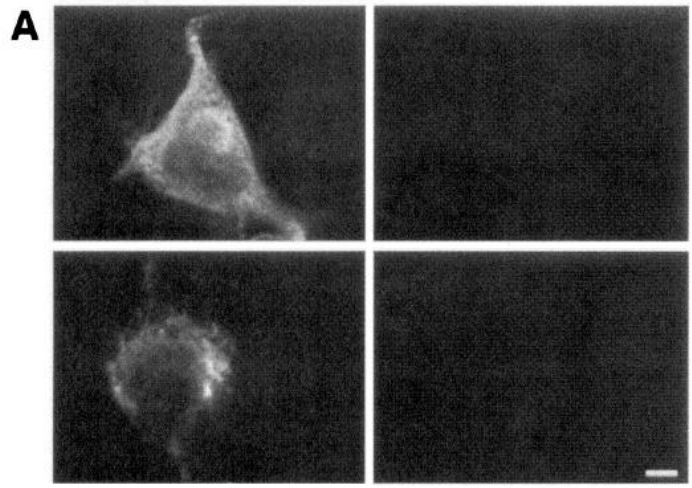

Figure 2. Characterization of a polyclonal antibody against IRK channels. *A*, Antiserum (anti-IRK) raised against a peptide sequence from the N-terminal cytoplasmic domain of IRK1 stains COS cells transfected with either IRK1 (*top left*) or IRK3 clones (*bottom left*). When the antibody was preabsorbed with the peptide immunogen, the staining of COS cells transfected with IRK1 and IRK3 was blocked (*top* and *bottom right*, respectively). Scale bar, 10 mm. *B*, Sequence comparison of the IRK1 peptide used for immunization with the homologous regions of rIRK2 and human IRK3. Identical residues are indicated with *double dots*; gaps are marked with *dashes*. *C*, Western blot of proteins from rat sciatic nerves (*lanes 1*, *3*, *4*) and brain (*lane 2*). Anti-IRK recognizes a 71 kDa and a 73 kDa band in sciatic nerve (*lane 1*) and in brain (*lane 2*), which may represent IRK1 and IRK3, respectively. An 81 kDa band is also detected in brain (*lane 2*). The immunoreactivity in sciatic nerve could be blocked by preabsorption of the antiserum with the immunogen (*lane 3*), and the bands were not seen in the absence of primary antibody (*lane 4*). Molecular weight standards (in kDa) are shown.

magnification the presence of bright puncta right at the nodal gap suggested staining of the microvilli, also called nodal processes, that occupy this space (Fig. 3*D*, *E*). IRK immunoreactivity was also observed in the perinuclear region (Fig. 3*B*) in what appeared to be predominantly intracellular pools.

Both nodal and perinuclear staining could be blocked by preincubating the antiserum with the N-terminal peptide immunogen (data not shown) but not with an unrelated peptide from the C-terminal region. Preimmune serum, although it showed some general background staining, did not mimic the affinity-purified anti-IRK pattern (data not shown).

We occasionally detected the axonal staining by anti-IRK in the vicinity of the node. The staining generally looked cytoplasmic and decreased to undetectable levels toward the paranodal and juxtaparanodal regions (data not shown). The staining occurred in only 10–20% of the nodes, but appeared to be specific because it, too, could be blocked by preincubation with the peptide immunogen. The heterogeneity of staining may reflect the heterogeneity of axons in the sciatic nerve. The heterogeneity is probably not caused by poor penetration of the antibodies, because similar results were obtained in 8 μm cryostat sections of nerves.

No IRK staining was detected in canaliculi, paranodal loops, the juxtaparanode, internode, or Schmidt–Lanterman incisures of Schwann cells; neither was any detected in paranodal, juxtaparanodal, or internodal regions of the axonal membrane.

To analyze the nodal staining more closely, immunoelectron microscopy was performed (Fig. 4). Consistent with the fluorescent cytochemistry, the IRK staining in the electron microscope was highly concentrated at the node and, indeed, seemed to occupy much of the nodal cleft to either side of the axon, where the microvilli are known to occur (Fig. 4*A*). At higher magnifications, individual microvilli can be seen that are clearly labeled by the antiserum (Fig. 4*B*). The structure of these immunoreactive processes can be discerned most clearly in stereo pairs of semithick sections (Fig. 5). The microvilli are finger-like structures projecting from the outer-most layer of the Schwann cell membranes into the nodal gap (Mugnaini et al., 1977; Wiley and Ellisman, 1980; Ellisman et al., 1984; Ichimura and Ellisman, 1991). The microvilli occupy much of this area and are often in direct contact with the nodal axon membrane.

The diffusion of the diaminobenzidine reaction product makes it difficult to determine whether the immunoreactivity in small structures such as microvilli resides on the plasma membrane, as would be expected. However, the staining in the perinuclear region seemed to be on intracellular structures rather than on the plasma membrane (Fig. 4*C*) and suggests the presence of this protein in the endoplasmic reticulum or Golgi apparatus. No staining was observed consistently in canaliculi of the Schwann cells, where Kv1.5 has been reported previously (Mi et al., 1995).

DISCUSSION

In this study, we have examined the expression and localization of inwardly rectifying K^+ channels in mature rat Schwann cells. Our findings indicate that IRK1 and IRK3 are expressed in adult sciatic nerve and are concentrated in the nodal microvilli of the Schwann cells. These findings suggest a likely role for these K^+ channels in the physiology of saltatory conduction in myelinated nerve. In addition, these studies provide further evidence that a cell can fine-tune the physiological properties of particular membrane domains by restricting the regional distribution of its membrane proteins.

Previous electrophysiological recordings found inward rectifying K^+ currents in both cultured Schwann cells and the membranes of myelinating Schwann cells near nodes of Ranvier (Wilson and Chiu, 1990b). The density of the currents was much greater at the node than elsewhere in the Schwann cell. This electrophysiological observation is fully supported by the present findings, which refine the localization to the microvilli and identify

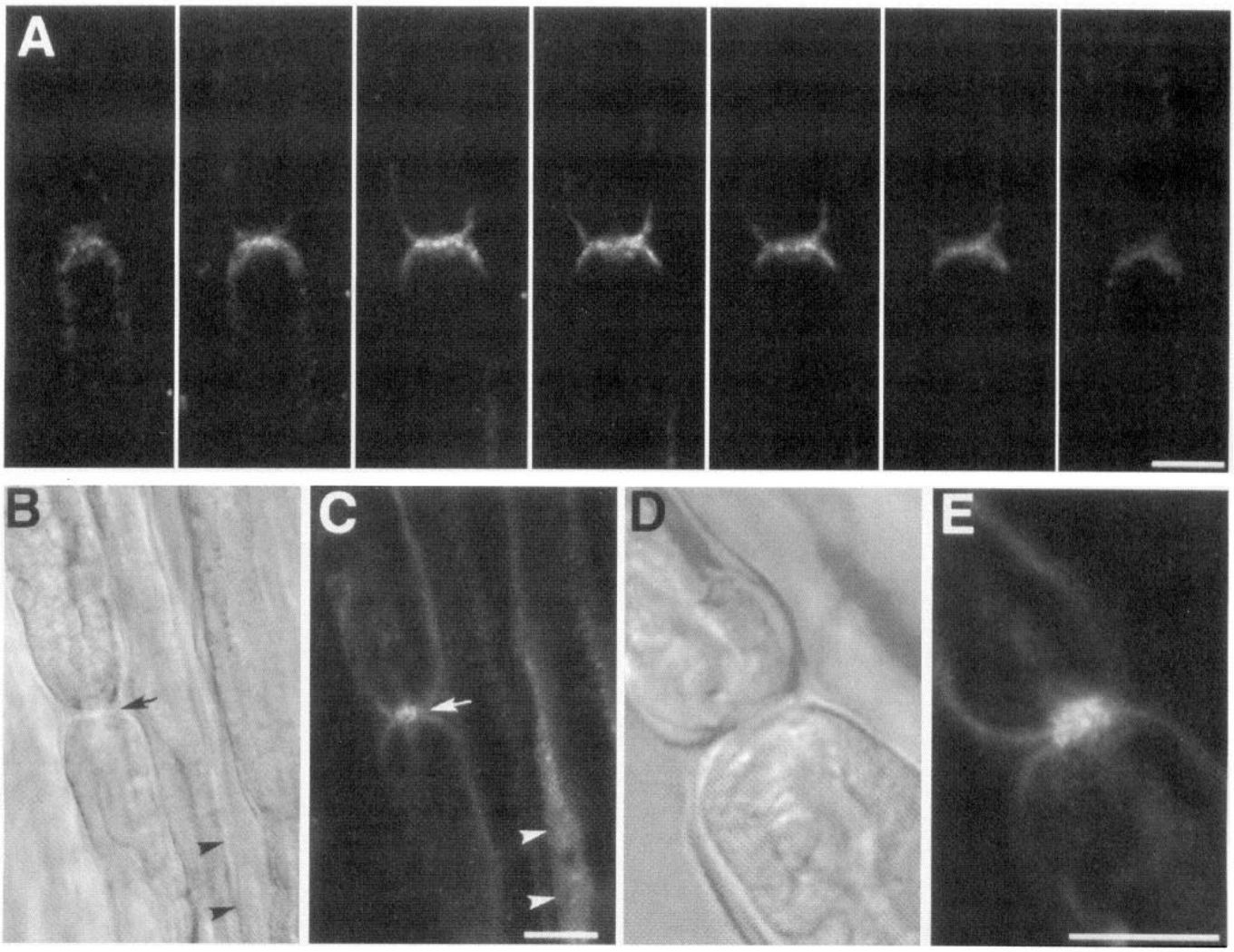

Figure 3. Immunofluorescent localization of IRK channels in adult rat sciatic nerves. *A*, Serial confocal optical sections of sciatic nerve stained by anti-IRK. A teased sciatic nerve was stained with anti-IRK. Immunoreactivity is highly concentrated at the node. No staining could be detected elsewhere on the surface of the Schwann cell. *B, C*, An immunostained node viewed in transmitted light optics (*B*) and in a confocal fluorescent section (*C*) to identify the region of channel expression. The node is indicated by an *arrow*. Staining can also be discerned in the perinuclear region of an adjacent Schwann cell (*arrowheads*). *D, E*, A high-magnification view of a stained node with Nomarski (*D*) and fluorescent imaging (*E*). The punctate staining in the immediate area of the node suggests that the nodal microvilli are labeled. Scale bars, 10 μm.

IRK1 and IRK3 as the molecular entities that are likely to carry the current.

It has been speculated that CNS glia and Schwann cells can take up K^+ and thereby help preserve the proper extracellular milieu in the face of K^+ efflux from active axons (Orkand et al., 1966; Barres et al., 1990a; Chiu, 1991). With regard to peripheral myelinated nerves, the likelihood of the K^+-buffering hypothesis is strengthened by the current findings. IRK channels are open at resting membrane potentials and favor the influx of ions. Their localization to the microvilli appears designed to maximize the surface area on which they contact the nodal space and also juxtaposes the channels to the axonal membranes, where the prevention of K^+ accumulation is most critical.

In our previous study, two delayed rectifiers were found to express in the Schwann cell (Mi et al., 1995), but it is unlikely that they participate in the uptake of K^+: they are further from the axon and, because they are open only at depolarized potentials, they allow K^+ efflux more easily than influx.

The location of the K^+ efflux from the axon during activity is not yet certain. The only K^+ channels to have been localized in myelinated axons are Kv1.1 and Kv1.2, which reside at the juxtaparanode (Wang et al., 1993; Mi et al., 1995) (see also Brau et al., 1990). Their significance for action potential repolarization is not certain, however; the very restricted extracellular space beneath the myelin that these channels open onto could not support a large movement of charge without causing a physiologically problematic accumulation of K^+. Although an as yet unidentified population of Schwann cell channels may take up these ions, there is little Schwann cell cytoplasm in this region and, therefore, little opportunity for K^+ uptake. Diffusion of the ions past the paranodal loops to the IRK channels in the nodal microvilli is possible but may be too slow to adequately buffer the juxtaparanodal space. Alternatively, the majority of the K^+ efflux in saltatory conduction may take place at the node itself via channels that have not yet been characterized molecularly or have not been recognized by the antibodies used so far. Indeed, physiological evidence suggests that much of the efflux is via a voltage-independent K^+ channel that causes a high resting permeability to

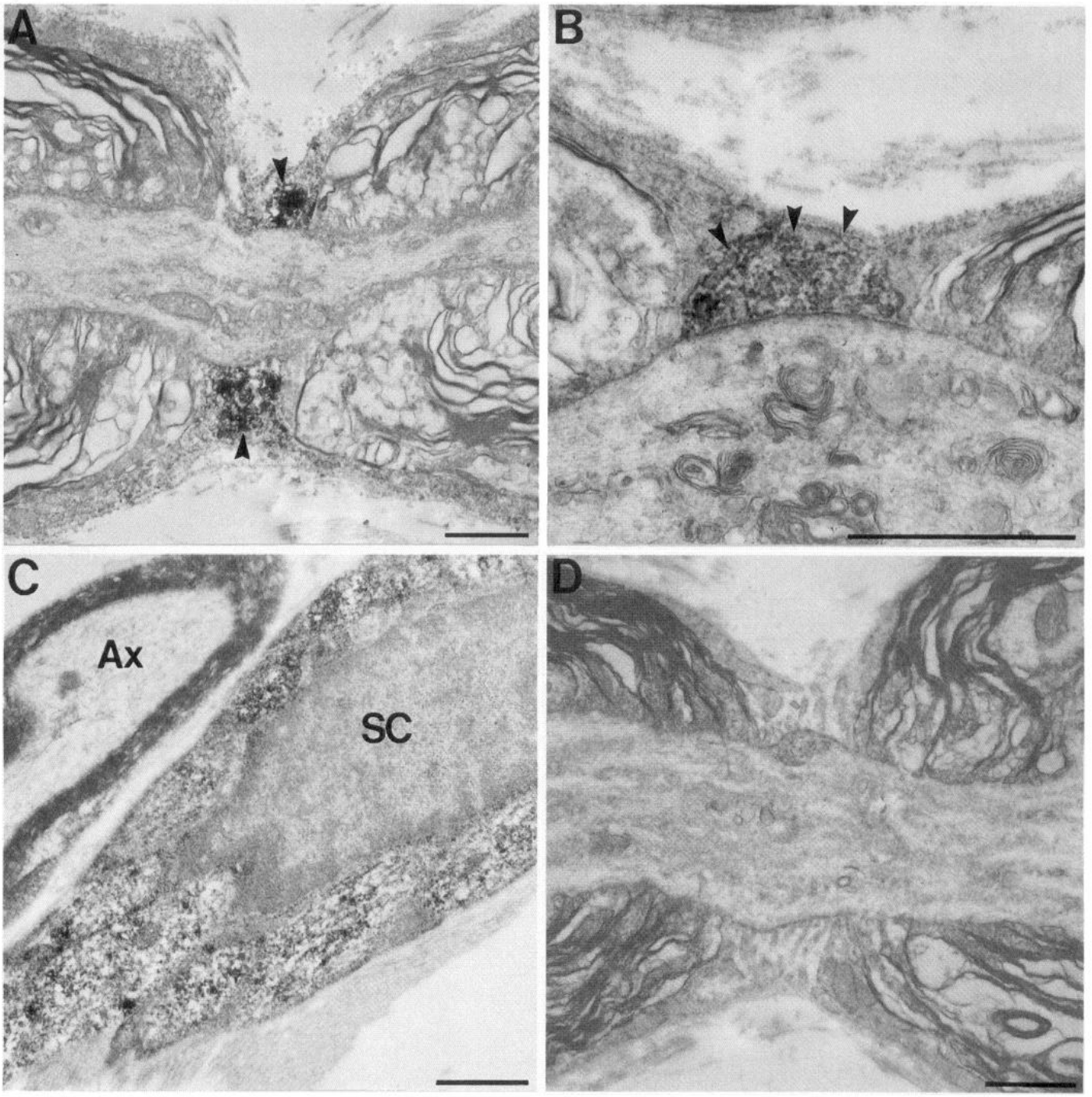

Figure 4. Immunoelectron microscopic study of IRK localization in Schwann cells. *A*, A node of Ranvier is shown at low magnification. The staining is seen in microvilli (*arrows*) that occupy much of the nodal gap and come in close contact with the axonal membrane. No staining was detected in other Schwann cell membranes or in axonal membranes. *B*, At higher magnification, individual microvilli are more apparent as finger-like structures (*arrows*) or round cross-sections, and the staining is associated with these structures. *C*, Intracellular punctate staining in the vicinity of the nucleus of a Schwann cell. *D*, In the absence of the primary antibody, no immunoreactivity was observed. Scale bars, 2 μm.

K^+ (Roper and Schwarz, 1989). This would be most consistent with the postulated role of the microvillar IRK channels in K^+ buffering.

Are IRK1 and IRK3 the channels recorded by Wilson and Chiu (1990b) on Schwann cell membranes near nodes? Their recordings from Schwann cells treated with collagenase to retract membranes probably would not have allowed the discrimination between the microvillar and paranodal compartments and, thus, the channels and the currents may indeed correspond. When expressed in oocytes, both IRK1 and IRK3 show strong inward rectification and sensitivity to Cs^+ and Ba^{2+} (Kubo et al., 1993a; Makhina et al., 1994; Perier et al., 1994). These properties also characterize the currents of Wilson and Chiu (1990b) as well as K^+ currents in astrocytes and retinal Müller cells (Brew et al., 1986; Barres et al., 1990b; Newman, 1993). The single-channel conductance of IRK1 is 21–22 pS (Kubo et al., 1993a; Takahashi et al., 1994), which is very close to the value of 25 pS reported for the Schwann cell channels (Wilson and Chiu, 1990b). The single-

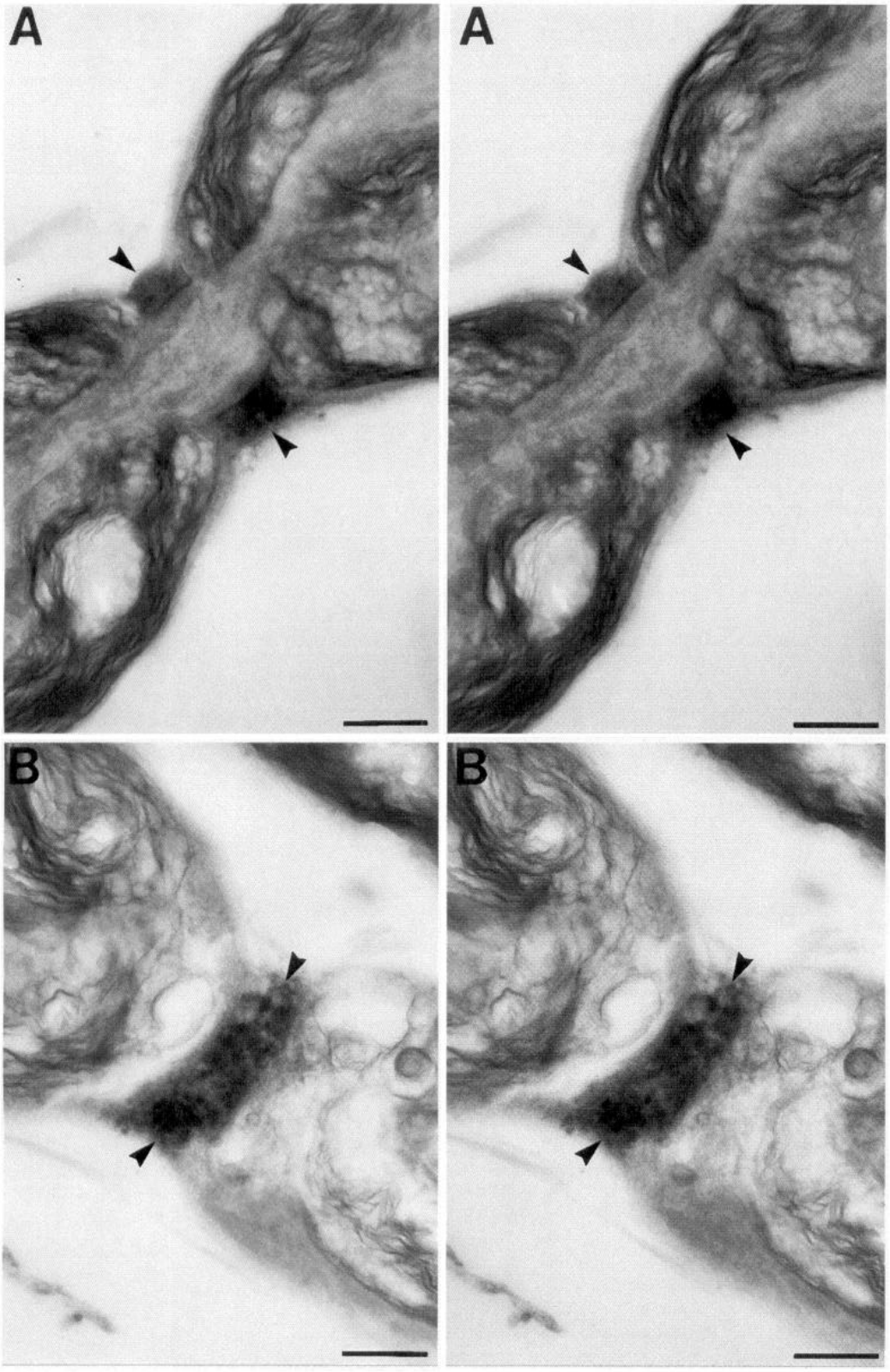

Figure 5. Anti-IRK staining in semi-thick sections of nodes of Ranvier. In stereo pair electron micrographs of semi-thick sections, the discrete nature of anti-IRK staining of the nodal microvilli can be appreciated (*arrows*). Three-dimensional images of thick sections provide a more complete view of the antigen distribution. Myelin that is electron dense but devoid of reaction product can be seen immediately adjacent to the stained regions. *A*, Stereo images through the central portion of a node of Ranvier. *B*, Stereo images of another node in a more tangential plane. Scale bars, 2 μm.

channel conductance of IRK3 is 10–13 pS (Makhina et al., 1994; Perier et al., 1994). IRK3 transcripts were less abundant than IRK1 in the sciatic nerve, and so these channels may be minor contributors to the current, perhaps coassembling with IRK1 subunits, and therefore may not be easily distinguished electrophysiologically.

With a more precise understanding of Schwann cell K^+ channels, it is now possible to revisit models of K^+ buffering in peripheral nerve. The resting membrane potential of the Schwann cell probably falls very close to the K^+ reversal potential, E_K. Thus, in a resting nerve there will be little net flow of K^+ through the IRK channels. During a period of activity in the axon, we anticipate a highly localized accumulation of K^+ immediately adjacent to the axon at the node. Because the accumulation covers

only a minute fraction of the Schwann cell surface, the resting potential of the Schwann cell will not be greatly affected. Nonetheless, E_K in the nodal microvilli will be shifted positively; if intracellular K^+ is 55 mM (Verkhratsky et al., 1991), a change in external K^+ from 4 to 6 mM will shift E_K by 11 mV. This shift of E_K away from the membrane potential is sufficient to cause an inward current through IRK channels.

Over time, this influx will cause a local depolarization of the nodal region of the Schwann cell that would pose a problem for sustained K^+ uptake. The coupling of this region of the cell, by the canaliculi, to regions that do not see elevated K^+ will help minimize the change in membrane potential. In essence, the canaliculi will decrease the input resistance of the nodal region of the Schwann cell, although we cannot predict by how much. Others have suggested that a Cl^- channel, by permitting Cl^- to follow the K^+, may also alleviate the depolarization. However, such a channel has not yet been identified or localized to this site (Barres et al., 1990b).

Another mechanism for maintaining the hyperpolarized membrane potential of the cell (and thereby the ability of the Schwann cells to take up K^+) is suggested by our knowledge of the distribution of the Kv1.5 channel in Schwann cells. If activated by the depolarization of the nodal region of the Schwann cell, this delayed rectifier will open and permit K^+ efflux along the surface of the Schwann cell at the edge of the node and in the canaliculi—areas somewhat removed from the immediate zone of elevated extracellular K^+. Thus, the spatial segregation of the inward rectifier and voltage activated channel may serve an important physiological function: to "syphon" K^+ from the immediate vicinity of the axon to the outside of the node.

It is interesting to note that the α_1 isoform of the Na^+/K^+ ATPase also localizes to the microvilli of Schwann cells (Ariyasu et al., 1985; Ariyasu and Ellisman, 1987). Like IRK channels, this pump may be important for the movement of K^+ ions: axonal activity that elevated K^+ and depleted Na^+ in the nodal extracellular space would favor Na^+ efflux from the Schwann cell with concomitant K^+ influx. Subsequently, the pump activity may be reversed and the Na^+ gradient could drive the efflux of K^+ from the microvilli so that K^+ can then be recaptured by the axon.

The inward rectifying K^+ channels in the microvilli of Schwann cells demonstrate again the precision with which a membrane protein can be localized by a cell. In a mature Schwann cell, numerous specialized membrane domains can now be recognized: the perinuclear region, myelin, canaliculi, outer Schwann cell membrane, nodal microvilli, paranodal loops or end feet, Schmidt–Lanterman incisures, and inner mesoaxon each appear molecularly distinct. The maintenance of these individual domains is presumably necessary for proper function of the cell. The differential distribution of Kv1.5 and the IRK channels at the node illustrates the degree of specialization that occurs and, as indicated above, this specialization may be crucial to nodal physiology. The localization of these channels strongly suggests a role in K^+ buffering and provokes new questions concerning the mechanisms by which these membrane domains are established and by which the precise distribution and density of these channels are maintained.

REFERENCES

Ariyasu RG, Ellisman MH (1987) The distribution of (Na^++K^+)ATPase is continuous along the axolemma of unensheathed axons from spinal roots of "dystrophic" mice. J Neurocytol 16:239–248.

Ariyasu RG, Nichol JA, Ellisman MH (1985) Localization of sodium/potassium adenosine triphosphatase in multiple cell types of the murine nervous system with antibodies raised against the enzyme from kidney. J Neurosci 5:2581–2596.

Ashford ML, Bond CT, Blair TA, Adelman JP (1994) Cloning and functional expression of a rat heart KATP channel. Nature 370:456–459.

Barres BA, Chun LY, Corey DP (1990a) Ion channels in vertebrate glia. Annu Rev Neurosci 13:441–474.

Barres BA, Koroshetz WJ, Chun LY, Corey DP (1990b) Ion channel expression by white matter glia: the type-1 astrocyte. Neuron 5:527–544.

Bevan S, Chiu SY, Gray PTA, Ritchie JM (1985) The presence of voltage-gated sodium, potassium and chloride channels in rat culture astrocytes. Proc R Soc Lond [Biol] 225:299–313.

Black JA, Kocsis JD, Waxman SG (1990) Ion channel organization of the myelinated fiber. Trends Neurosci 13:48–54.

Bond CT, Pessia M, Xia X-M, Lagrutta A, Kavanaugh MP, Adelman JP (1994) Cloning and expression of a family of inward rectifier potassium channels. Receptors Channels 2:183–191.

Brau ME, Dreyer F, Jonas P, Repp H, Vogel W (1990) A K channel in *Xenopus* nerve fibers selectively blocked by bee and snake toxins: binding and voltage-clamp experiments. J Physiol (Lond) 420:365–385.

Brew H, Gray PT, Mobbs P, Attwell D (1986) Endfeet of retinal glial cells have higher densities of ion channels that mediate K^+ buffering. Nature 324:466–468.

Brismar T, Collins VP (1989) Inward rectifying potassium channels in human malignant glioma cells. Brain Res 480:249–258.

Chiu SY (1991) Functions and distribution of voltage-gated sodium and potassium channels in mammalian Schwann cells. Glia 4:541–558.

Chiu SY, Shrager P, Ritchie JM (1984) Neuronal-type Na^+ and K^+ channels in rabbit cultured Schwann cells. Nature 311:156–157.

Doupnik CA, Davidson N, Lester HA (1995) The inward rectifier potassium channel family. Curr Opin Neurobiol 5:268–277.

Ellisman MH (1979) Molecular specializations of the axon membrane at nodes of Ranvier are not dependent upon myelination. J Neurocytol 8:719–735.

Ellisman MH, Wiley CA, Lindsey JD, Wurtz CC (1984) Structure and function of the cytoskeleton and endomembrane systems at the node of Ranvier. In: Cellular neurobiology: a series, the node of Ranvier (Zagoren J, Federoff S, eds), pp 153–181. New York: Academic.

Ho K, Nichols CG, Lederer WJ, Lytton J, Vassilev PM, Kanazirska MV, Hebert SC (1993) Cloning and expression of an inwardly rectifying ATP-regulated potassium channel. Nature 362:31–38.

Howe JR, Ritchie JM (1988) Two types of potassium currents in rabbit cultured Schwann cells. Proc R Soc Lond [Biol] 235:19–27.

Ichimura T, Ellisman MH (1991) Three dimensional fine structure of cytoskeletal-membrane interactions at nodes of Ranvier. J Neurocytol 20:667–681.

Konish T (1989) Voltage-dependent potassium channels in mouse Schwann cells. J Physiol (Lond) 411:115–130.

Koyama H, Morishige K-I, Takahashi N, Zanelli J, Fass DN, Kurachi Y (1994) Molecular cloning, functional expression and localization of a novel inward rectifier potassium channel in the rat brain. FEBS Lett 341:303–307.

Krapivinsky G, Gordon EA, Wickman K, Velimirovic B, Krapivinsky L, Clapham DE (1995) The G-protein-gated atrial K^+ channel I_{KACh} is a heteromultimer of two inward rectifying K^+-channel proteins. Nature 374:135–141.

Kubo Y, Baldwin TJ, Jan YN, Jan LY (1993a) Primary structure and functional expression of a mouse inward rectifier potassium channel. Nature 362:127–133.

Kubo Y, Reuveny E, Slesinger PA, Jan YN, Jan LY (1993b) Primary structure and functional expression of a rat G-protein-coupled muscarinic potassium channel. Nature 364:802–806.

Makhina EN, Kelly AJ, Lopatin AN, Mercer RW, Nichols CG (1994) Cloning and expression of a novel human brain inward rectifier potassium channel. J Biol Chem 269:20468–20473.

Mi H, Deerinck TJ, Ellisman MH, Schwarz TL (1995) Differential distribution of closely related potassium channels in rat Schwann cells. J Neurosci 15:3761–3774.

Monuki ES, Weinmaster G, Kuhn R, Lemke G (1989) SCIP: a glial POU domain gene regulated by cyclic AMP. Neuron 3:783–793.

Morishige K, Takahashi N, Jahangir A, Yamada M, Koyama H, Zanelli JS, Kurachi Y (1994) Molecular cloning and functional expression of a novel brain-specific inward rectifier potassium channel. FEBS Lett 346:251–256.

Mugnaini E, Osen KK, Schnapp B, Friedrich VL Jr (1977) Distribution of Schwann cell cytoplasm and plasmalemmal vesicles (caveolae) in

peripheral myelin sheaths: an electron microscopic study with thin section and freeze-fracturing. J Neurocytol 6:647–668.
Newman EA (1993) Inward-rectifying potassium channels in retinal glial (Müller) cells. J Neurosci 13:3333–3345.
Orkand RK, Nicholls JG, Kuffler SW (1966) Effect of nerve impulses on the membrane potential of glial cells in the central nervous system of amphibia. J Neurophysiol 29:788–806.
Perier F, Radeke CM, Vandenberg CA (1994) Primary structure and characterization of a small-conductance inward rectifying potassium channel from human hippocampus. Proc Natl Acad Sci USA 91:6240–6244.
Ritchie JM (1992) Voltage-gated ion channels in Schwann cells and glia. Trends Neurosci 15:345–351.
Roper J, Schwarz JR (1989) Heterogeneous distribution of fast slow potassium channels in myelinated rat nerve fibers. J Physiol (Lond) 416:93–110.
Rosenbluth J (1979) Aberrant axon-Schwann cell junctions in dystrophic mouse nerves. J Neurocytol 8:655–672.
Sambrook J, Fritsch EF, Maniatis T (1989) Molecular cloning: a laboratory manual. Cold Spring Harbor, NY: Cold Spring Harbor Laboratory.
Shrager P, Chiu SY, Ritchie JM (1985) Voltage-dependent sodium and potassium channels in mammalian cultured Schwann cells. Proc Natl Acad Sci USA 82:948–952.
Takahashi N, Morishige K-I, Jahangir A, Yamada M, Findley I, Koyama H, Kurachi Y (1994) Molecular cloning and functional expression of cDNA encoding a second class of inward rectifier potassium channels in the mouse brain. J Biol Chem 269:23274–23279.
Tang W, Yang X-C (1994) Cloning a novel human brain inward rectifier potassium channel and its functional expression in *Xenopus* oocytes. FEBS Lett 348:239–243.
Verkhratsky A, Hoppe D, Kettenmann H (1991) Single K^+ channel properties in cultured mouse Schwann cells: conductance and kinetics. J Neurosci Res 28:200–209.
Villegas J (1981) Axon/Schwann-cell relationships in the giant nerve fiber of the squid. J Exp Biol 95:135–151.
Wang H, Kunkel DD, Martin TM, Schwartzkroin PA, Tempel BL (1993) Heteromultimeric K^+ channels in terminal and juxtaparanodal regions of neurons. Nature 365:75–79.
Wiley CA, Ellisman MH (1980) Rows of dimeric-particles within the axolemma and juxtaposed particles within glia incorporated into a new model for the paranodal glial-axonal junction at the node of Ranvier. J Cell Biol 84:261–80.
Wiley-Livingston C, Ellisman MH (1980) Development of axonal membrane specializations defines nodes of Ranvier and precedes Schwann cell myelin elaboration. Dev Biol 79:334–355.
Wiley-Livingston CA, Ellisman MH (1981) Myelination-dependent axonal membrane specializations demonstrated in insufficiently myelinated nerves of the dystrophic mouse. Brain Res 224:55–67.
Wilson GF, Chiu SY (1990a) Regulation of potassium channels in Schwann cells during early development of myelinogenesis. J Neurosci 10:1615–1625.
Wilson GF, Chiu SY (1990b) Ion channels in axon and Schwann cell membrane at paranodes of mammalian myelinated fibers studied with patch clamp. J Neurosci 10:3263–3274.